IMPLEMENTATION OF A TWO DIMENSIONAL PLANE WAVE FDTD USING ONE DIMENSIONAL FDTD ON THE LATTICE EDGES

Scott C. Winton and Carey M. Rappaport
Center for Electromagnetics Research
Northeastern University
Boston, MA 02115

Abstract **Development and testing of angle independent absorbing boundary conditions (ABCs) can be improved by simulating waves incident on the ABC at a single angle. By using one-dimensional Finite Difference Time Domain (FDTD) as the lattice side edge condition, the creation and numerical propagation of a two dimensional plane wave with arbitrary incident angle is possible. The application and extent of usefulness of the method are examined and extensions to increase the range of usefulness are introduced.**

I. INTRODUCTION

Until recently, the use of the FDTD method for numerical solutions of electromagnetic scattering problems was severely hampered by the poor performance of absorbing boundary conditions used to prevent reflections of EM waves at the lattice edges. With the advent of the Berenger Perfectly Matched Layer[1], this problem has been significantly reduced and the computational efficiency of FDTD problems has been significantly improved.

Understandably, this has created considerable interest in improving and optimizing the PML and angle-independent ABCs as a whole. But this effort has been impaired by the fact that commonly used excitations, such as point or line sources, generate waves incident on the ABC at all angles. This complicates the analysis of the performance of the ABC and impairs design optimization. The problem is ameliorated by introducing plane wave sources incident on the ABC at a single angle. With such an excitation, the performance of the ABC is clearly defined. However, because of the difficulty in dealing with propagation on the lattice edge ,the creating and propagating such a wave is difficult.

For a two-dimensional FDTD simulation using the standard Yee cell formulation[2], the update of a given spatial grid point requires data from the four adjacent grid points. Clearly this creates a problem at the lattice edges. Typically, in scattering simulations, a Mur total/scattered field region separation avoids the need to calculate incident waves on the edges[3]. However, to test ABCs, the incident wave must be a uniform plane wave without deformations along the edge. ABCs cannot be used at these edges since they fail for plane waves propagating at steep grazing angles. Furthermore, the values on the edges must not be specified analytically because the numerical values of the fields inside the discretized ABC under test are not known.

II. INTEGRATION OF ONE-DIMENSIONAL EDGE FDTD WITH A TWO-DIMENSIONAL GRID

For the following discussion, consider a two-dimensional grid on which a boundary value FDTD simulation will be run. The "front" of the grid is the source boundary value while the ABC to be tested is positioned at the "back". What is desired is the create a plane wave with a phase front at an angle θ with respect to the front wall. For this discussion a transverse electric (TE) wave is considered. The x directions is front to back and the y direction is left to right as shown in Figure 1.

Instead of ABCs at the "left" and "right" edges, 1-D FDTD is used. The update of each spatial point on these edges will require data from only the grid points preceding and succeeding it. At each time step, information from this 1-D FDTD is passed to the larger 2-D FDTD to update spatial points adjacent to the left and right edges. If the wave is normally incident on the ABC, the formulation of the plane wave is quite simple. In this case, H_x is zero and both E_z and H_y are uniform left to right. Therefore, no information is obtained from the transverse difference and the calculations along each grid line running front to back reduces to as a 1-D FDTD algorithm. To illustrate this, consider the time harmonic Maxwell's curl equations for TE waves in lossless media:

$$\frac{\partial E_z}{\partial y} = -j\omega\mu H_x \tag{1a}$$

$$\frac{\partial E_z}{\partial x} = j\omega\mu H_y \tag{1b}$$

$$\frac{\partial H_y}{\partial x} + \frac{\partial H_x}{\partial y} = j\omega\epsilon E_z \tag{1c}$$

These have the familiar (forward propagating) solutions:

$$E_z = E_o e^{-jk(x\cos\theta + y\sin\theta)} \tag{2a}$$

$$H_y = -\cos\theta \frac{E_o}{\eta} e^{-jk(x\cos\theta + y\sin\theta)} \tag{2b}$$

$$H_x = -\sin\theta \frac{E_o}{\eta} e^{-jk(x\cos\theta + y\sin\theta)} \tag{2c}$$

It is clear that for normal incidence, ($\theta = 0$), this becomes a TEM wave with no y dependence. Equations (1a) and (2c) become unnecessary and the 1-D FDTD and the 2-D FDTD calculations are identical.

The situation is more complicated when θ is nonzero. Now H_x is nonzero and the 1-D wave is no longer identical to the 2-D wave. In order for the 1-D FDTD simulation to supply the correct data to the 2-D grid, the 1-D wave must propagate with a velocity that keeps pace with the 2-D wave. This velocity is simply the phase velocity of the 2-D wave in the x direction, *i.e.* $v_{1D} = v_o/cos\theta$, where v_o is the velocity of the 2-D wave in the direction θ. This is analogous to taking a slice along the right (or left) edge of the grid, of an infinite 2-D plane wave. Clearly this "slice" must travel along the edge with greater velocity than the the wave traveling an angle θ. Since the velocity, v_{1D} of this wave is given as $v_{1D} = \frac{\omega}{k_x}$, we can write Eq. (2) for the 1-D wave at $y = 0$ as:

$$E_{z_{1D}} = E_o e^{-jkx\cos\theta} \tag{3}$$

$$H_{y_{1D}} = -\cos\theta \frac{E_o}{\eta} e^{-jkx\cos\theta}$$

The solution in Eq.(3) does not satisfy Maxwell's curl equations. This problem can be addressed by modifying Ampere's Law. By taking the partial derivative of Eq.(2c) at $y = 0$ one obtains:

$$\frac{\partial H_x}{\partial y} = jk\sin^2\theta \frac{E_o}{\eta} e^{-jkx\cos\theta},$$

which, using Eq.(2b) becomes

$$\frac{\partial H_x}{\partial y} = \frac{(1-\cos^2\theta)\frac{\partial H_y}{\partial x}}{\cos^2\theta}.$$

Thus,

$$\frac{\partial H_y}{\partial x} + \frac{\partial H_x}{\partial y} = \frac{1}{\cos^2\theta}\frac{\partial H_y}{\partial x}$$

Now Eq.(1), for the 1-D wave will become:

$$\frac{\partial E_{z_{1D}}}{\partial x} = j\omega\mu H_{y_{1D}} \tag{4}$$

$$\frac{1}{\cos^2\theta}\frac{\partial H_{y_{1D}}}{\partial x} = j\omega\epsilon E_{z_{1D}}$$

Having described the changes to Maxwell's equations needed to integrate the 1-D FDTD into the 2-D grid, it is worthwhile examining the discretization of the modified 1D curl equations.

III. DISCRETIZATION OF MODIFIED EQUATIONS AND STABILITY CONSIDERATIONS

Through a straight forward discretization process[4], the discretized 1-D modified Maxwell's curl equations for lossless media become;

$$E_i^{n+\frac{1}{2}} = E_i^{n-\frac{1}{2}} + \frac{R}{\cos^2\theta}\eta({H^n}_{i+\frac{1}{2}} - {H^n}_{i-\frac{1}{2}}) \tag{5}$$

$${H^{n+1}}_{i+\frac{1}{2}} = {H^n}_{i+\frac{1}{2}} + \frac{R}{\eta}(E_{i+1}^{n+\frac{1}{2}} - E_i^{n+\frac{1}{2}})$$

where n is the time index, i is the space index and $R = v_o\Delta t/\Delta x$ is the Courant Number, and the vector component designations has been suppressed. Note that the velocity of the modified 1-D wave is $v_{1D} = \frac{v_o}{\cos\theta}$ as is apparent in the discretized wave equation based on Eq.(5).

Of particular importance is the Courant Number, R. Stability analysis indicates that for a FDTD simulation to be stable $R \leq 1$. For Equation (5), a new Courant number $R_{1D} = \frac{R}{\cos\theta}$ must be used instead. Since $R_{1D} \leq 1$, the usefulness of this method is limited to smaller angles. For example, let R_g be the Courant Number of the 2-D FDTD simulation. If R_g is chosen to be 0.5, then the largest angle that may be used is 60°. Clearly larger angles may be used if R_g is chosen to be smaller. However, since R_g is also a measure of how fast the wave moves through the grid, choosing it too small increases computational expense for the entire 2-D grid.

IV. LARGE ANGLE SOLUTIONS

For applicability with large propagation angles without decreasing R_g, changes must be made to the method. This is done by adjusting the Courant Number of the 1-D FDTD edge simulation. A smaller Courant number $R'_{1D} = v_o\Delta t'/\Delta x\cos\theta$ may be chosen such that $R'_{1D} \leq R_{1D}$. Since Δx remains the same, two simulations using R'_{1D} and R_{1D} would be spatially similar at the same physical time t, whenever $n'\Delta t' = n\Delta t$ for some different number of new time steps. The the stability condition is now $R'_{1D} \leq 1$ and thus θ may be increased.

Some care must be exercised in order to insure that the correct data is being passed to the 2-D grid. Let $m = \Delta t/\Delta t'$. If m is an integer$(= n'/n)$, then the m^{th} iteration of the 1-D FDTD is used to update the 2-D interior of the grid. If m is not an integer, then the correct value of E_z on the edge of the lattice must be interpolated with respect to time from two or more iterations of the 1-D FDTD and **then** supplied to the 2-D grid.

The interpolation process is quite straight forward, with emphasis given to insuring the correct timing. Assume the 1-D FDTD simulation has a time sample interval of $\Delta t'$ and the 2-D simulation has a time sample interval of Δt. To meet the above criteria, $\Delta t' \leq \Delta t$. In order to insure that interpolation, and not extrapolation, is being performed, the 1-D simulation must be performed until $n'\Delta t' \geq n\Delta t$. The number of previous time values that must be stored in order to perform the interpolation is equal to the order of interpolation desired. Increasing the order will increase accuracy, but since previous values must be stored for **every** point on the 1-D grid, the order should be kept as low as possible.

Once the values needed for interpolation have been identified and calculated, any standard interpolation algorithm, such as Lagrange Interpolation, can be used. After the interpolated edge E_z values have been calculated, they can then be supplied to the 2-D grid. The edge H_y values need not be interpolated.

V. FDTD SIMULATION RESULTS

Several experiments were performed using the methods described above using a variety of parameters. Excellent results were obtained for angles ranging from 0 to 85 degrees. The general method of each experiment was the same. A Gaussian pulse plane wave was created along the initial boundary at $x = 0$ with time variation corresponding to various propagation angles and with various values of R_g. In each of these experiments, the plane wave encounters a PML ABC at the back of the grid. The ABC in question is from [5] with 8 PML layers and conductivity profile $\sigma_i = \sigma_f(i/8)^{3.7}$. Figure 2a shows a 50×50 view sampled from a 200×200 grid. The propagation angle is 45° degrees and the Courant Number R_g is 0.5. Note that the wave propagates without edge distortion. Figure 2b is the same wave 200 time steps later. The wave has encountered the ABC and no reflection is visible, even in the lattice corner, where the 1-D FDTD accurately extends the 2-D ABC interaction calculation to the edge. In the scattered field view 2c, which is at the same time step as 2b, the magnification has been increased by 5 orders of magnitude and the incident field has been removed. The features to note are that the scattered wave satisfies Snell's law and that the scattered wave is uniform along the 45° angle, *i.e.*, the introduction of the 1-D FDTD on the right edge of the grid has not introduced any additional reflection artifacts. Figure 3a is once again a 50×50 view of a 200×200 grid. Here the Gaussian pulse plane wave is incident on the ABC at 70°. Once again R_g is 0.5 but now $R_s{}' = 0.25/\cos\theta$. The 1-D wave is traveling at one-half the velocity needed to keep pace with the 2-D wave, so only every second time sample is passed to the 2-D grid. Figure 3b is the same wave 150 time steps later. As with 45° wave, the interaction with the ABC has produced no visible reflection. Once again it may be noticed that the scattered wave, Figure 3c, obeys Snell's law and is uniform along the Snell angle. Clearly the visible reflection is due solely to the plane wave interacting with the ABC, which is the desired information.

VI. CONCLUSIONS

A method for testing angle-independent ABCs has been described. By using a one-dimensional FDTD simulation on the left and right edges of a two-dimensional grid, a plane wave incident on a ABC at the back edge of the grid at a single angle can be created and propagated. This method will greatly simplify the analysis of angle-independent ABC performance. The method has been tested using a Gaussian pulse plane wave with a variety of parameters and has been shown to give excellent results. Finally, since all of the desired information is found in the 1-D simulations, it can be concluded that the analysis of angle-independent ABCs may be carried out using only 1-D simulations.

REFERENCES

[1] Berenger, J., "A Perfectly Matched Layer for the Absorption of Electromagnetic Waves", *Journal of Computational Physics*, Vol. 114, No. 1, pp. 185–200, October 1994.

[2] Yee K.S., "Numerical Solution of Initial Boundary-Value Problems Involving Maxwell's Equations in Isotropic Media", *IEEE Trans. Ant. Prop.*, Vol. AP-14, No. 1, pp. 302–307, May 1966.

[3] Mur, G., "Absorbing Boundary Conditions for the Finite-Difference Approximation of the Time-Domain Electromagnetic-Field Equations", *IEEE Transactions on Electromagnetic Compatibility*, Vol. EMC-23, No. 4, pp. 377–382, November 1981.

[4] Sadiku, M.N.O, "Numerical Techniques in Electromagnetics", pp. 139–144, CRC Press, Boca Raton, 1992.

[5] Rappaport, C., "Interpreting and Improving the PML Absorbing Boundary Condition Using Ansitropic Lossy Mapping of Space", *IEEE Trans. on Magnetics*, pp. 968–974, May 1996.

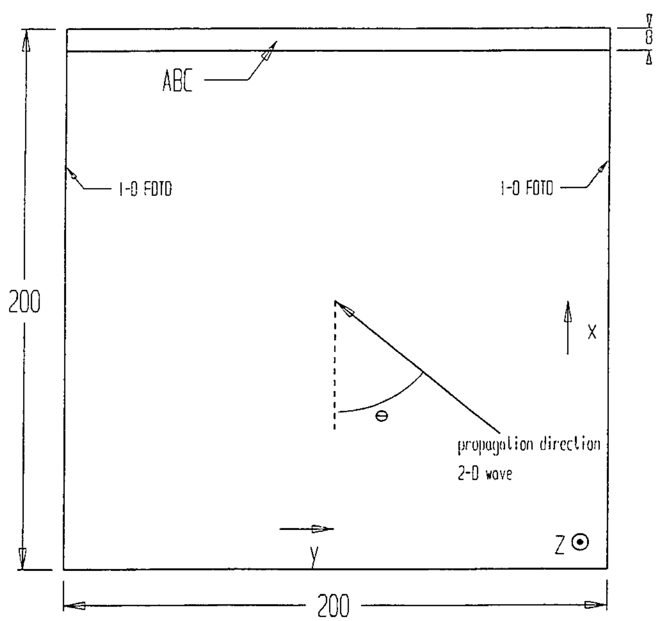

Figure 1
Geometry of grid.

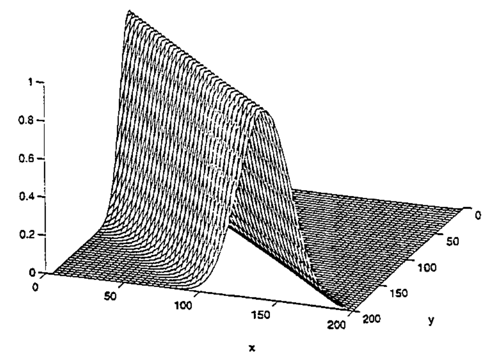

Figure 2a Gaussian pulse plane wave generated at $x = 0$ incident on the ABC at 45°. After 500 time steps, the 1-D FDTD simulation at $y = 200$ aligns perfectly with the 2-D FDTD simulation throughout the grid. ABC exists for $192 \leq x \leq 199$.

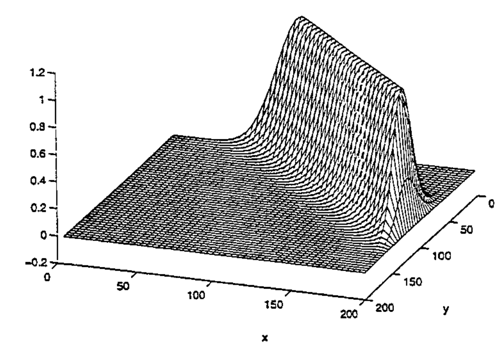

Figure 2b Gaussian pulse of Figure 2a, 200 time steps later: total field. The pulse has encountered the ABC, and is almost completely absorbed.

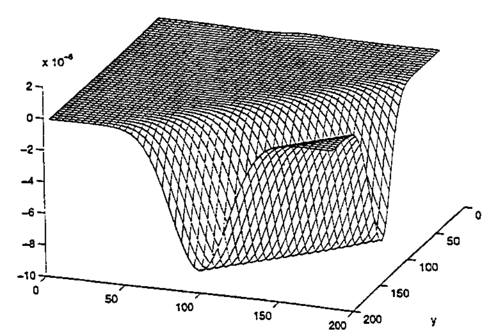

Figure 2c Scattered field at the same time of Figure 2b showing the residual reflection of the ABC.

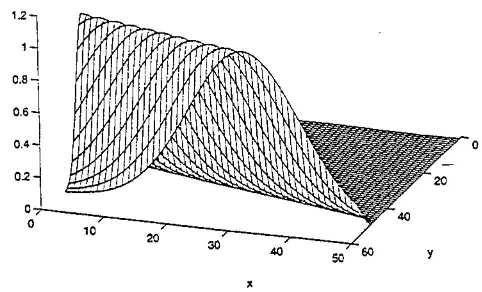

Figure 3a Gaussian pulse plane wave generated at $x = 0$ incident on the ABC at 70°. After 375 time steps, the 1-D FDTD simulation at $y = 200$ aligns perfectly with the 2-D FDTD simulation throughout the grid. ABC exists for $192 \leq x \leq 199$.

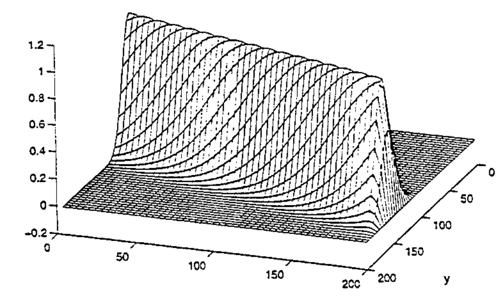

Figure 3b Gaussian pulse of Figure 3a 150 time steps later: total field.The pulse has encountered the ABC and is almost completely absorbed.

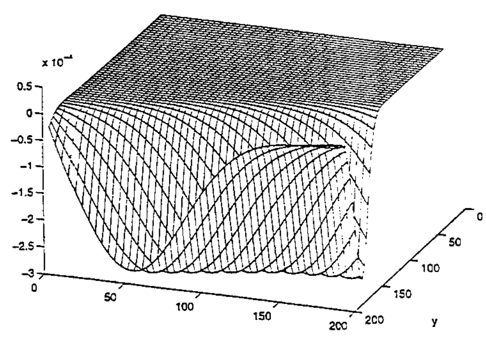

Figure 3c Scattered field at the same time of Figure 3b showing the residual reflection of the ABC.